separations

MDPI

Article

Separation of Residual Combustible Matter from Coal Gasification Fine Slag Using a Combined Supergravity-Sieving Process Enhanced by Ultrasonic Dispersion

Jingfeng He [1,2,3,4,*], Liangyu Yao [3,4], Yangge Zhu [1,*], Lingtao Zhu [3,4] and Yuhao Liu [3,4]

[1] State Key Laboratory of Mineral Processing, BGRIMM Technology Group, Beijing 100160, China
[2] Key Laboratory of Xinjiang Coal Resources Green Mining, Ministry of Education, Xinjiang Institute of Engineering, Urumqi 830023, China
[3] School of Chemical Engineering and Technology, China University of Mining and Technology, Xuzhou 221116, China; ltzhu@cumt.edu.cn (L.Z.)
[4] Key Laboratory of Coal Processing & Efficient Utilization (China University of Mining and Technology), Ministry of Education, Xuzhou 221116, China
* Correspondence: jfhe@cumt.edu.cn (J.H.); zhuyangge@bgrimm.com (Y.Z.)

Abstract

The resource utilization of coal gasification fine slag (CGFS) is critical for reducing solid waste and promoting its high-value use in the coal chemical industry. To address the challenge of tight interlocking between residual combustible matter (coke) and glass microspheres, which limits the effectiveness of conventional physical separation, this study proposes a combined supergravity-sieving separation process enhanced by ultrasonic dispersion. The effects of the strong mechanical shear force generated by ultrasonic cavitation on the disaggregation and surface cleaning of heterogeneous agglomerates in CGFS were systematically investigated, and the settling separation mechanism of the liberated particles in the centrifugal field was examined. The experimental results demonstrate that ultrasonic pretreatment can disrupt the physical encapsulation and agglomeration constraints between combustible matter and ash particles, creating favorable prerequisites for efficient separation in the subsequent supergravity field. Under the optimized pretreatment conditions, the loss on ignition (LOI) of the final concentrate obtained by the combined ultrasonic-supergravity-sieving process was 84.04%, which was 18.52% higher than that from supergravity separation alone. Furthermore, with the addition of wet sieving, the micro-fine inorganic ash liberated by ultrasonication was effectively removed, contributing to the enrichment and recovery of residual combustible matter. This study provides microscopic evidence consistent with the proposed mechanism of the combined process and offers a feasible technical pathway for the efficient recovery of valuable combustible matter from CGFS.

Keywords: coal gasification fine slag; combustible matter-ash separation; ultrasonic dispersion; supergravity separation; residual combustible matter recovery

Check for updates

Academic Editor: Xiong Yang

Received: 4 September 2026
Revised: 20 October 2026
Accepted: 22 October 2026
Published: 24 October 2026

Copyright: © 2026 by the authors. Licensee MDPI, Basel, Switzerland. This article is an open access article distributed under the terms and conditions of the Creative Commons Attribution (CC BY) license.

1. Introduction

Coal gasification technology serves as a crucial pathway for clean coal utilization; however, it generates large amounts of solid waste in the form of coal gasification slag, whose annual production in China reaches tens of millions of tons [1]. If coal gasification slag is stockpiled without proper treatment, it not only causes a waste of resources but also threatens the ecological environment through dust and leachate [1,2]. Therefore, the

reduction and harmless disposal of coal gasification slag are vital for the comprehensive utilization of coal resources [3,4]. The fine slag fraction (CGFS) has considerable resource recovery potential because of its relatively high content of residual combustible matter [5,6]. Currently, froth flotation and conventional gravity separation are the primary methods for combustible matter-ash separation in fine slag [7–9]. Flotation is constrained by the complex surface properties of the fine slag, resulting in high reagent consumption and poor selectivity [10,11]. In contrast, conventional gravity separation has garnered attention because of its low cost and environmental friendliness; however, its application is significantly restricted by the minimum treatable particle size, resulting in low separation precision when treating fine particles [5,7]. Consequently, overcoming the particle size limitations of conventional physical separation necessitates the introduction of novel high-precision equipment. However, addressing these particle size constraints alone is insufficient to effectively separate combustible matter from ash. Given the robust physical encapsulation between the residual combustible matter and inorganic ash, an effective separation method must combine intense mechanical action to break the combustible matter-ash intergrowths with an enhanced force field to promote density-based stratification.

Supergravity separation technology provides a novel approach for the efficient separation of fine particles by generating an intensified force field much stronger than that generated by conventional gravity, effectively increasing the differences in settling velocity between particles [5]. Nevertheless, studies indicate that CGFS commonly contains combustible matter-ash intergrowths with strong adhesion and a high proportion of interlocked particles. Because of this robust physical encapsulation, an intensified force field alone is insufficient to achieve deep component liberation [12,13]. To address this limitation, ultrasonic pretreatment has gained attention due to its unique mechanical effects. The rapid collapse of ultrasonic cavitation bubbles releases intense localized shock waves and strong mechanical shear forces, which can break down mineral agglomerates, liberate components, and clean particle surfaces [14–16]. Recent studies have demonstrated that ultrasonication can effectively disrupt the physical constraints of CGFS [11,14]. However, ultrasonic treatment alone merely disperses the interlocked particles; the liberated micro-fine ash and other fine impurities remain in the slurry and may be entrained in the overflow product during subsequent supergravity separation. Therefore, introducing a wet sieving step can further purify the overflow concentrate by removing these impurities, thereby reducing ash contamination and improving the quality of the final combustible-matter-rich product.

Previous studies provide valuable references for the process proposed herein. Kundu et al. [17] investigated tungsten recovery from gold tailings via enhanced-gravity concentration, while Silva, G.V. et al. [18] examined ultrasound-assisted Bauxite flotation. For CGFS, Lv et al. [13] combined gravity separation and flotation; Han et al. [11] coupled classification and ultrasonication with flotation; Sun et al. [15] adopted ultrasonic pretreatment prior to wet sieving. Recent research has explored ultrasound-assisted flotation and hydrophobic–hydrophilic separation [19,20], centrifugal airflow classification [21], supergravity treatment of coarse gasification slag [22], combined gravity–magnetic separation [23], and integrated sieving–water flow classification [24]. Variations in feed properties and carrier phases restrict direct quantitative comparison of separation performance. Most of these investigations focus on single unit operations or alternative process combinations. By contrast, the present work constructs a unified four-test scenario framework to systematically examine the coupled workflow integrating ultrasonic dispersion, supergravity separation and subsequent wet sieving specifically for CGFS.

Against this background, this study proposes an ultrasonic dispersion-enhanced supergravity-sieving separation process to tackle the critical separation bottleneck arising from tight interlocking and physical encapsulation between residual combustible matter

and glass microspheres in CGFS. Although the individual effects of ultrasonication or supergravity have been reported in prior literature, the synergistic mechanism linking ultrasonic cavitation-induced liberation, supergravity centrifugal stratification and post-separation sieving purification for CGFS has rarely been elucidated. The core novelty of this work lies in the tailored sequential integration of these mature unit operations for CGFS treatment. The four designed process configurations enable clear differentiation of the respective contributions of ultrasonic dispersion and downstream wet sieving under identical supergravity conditions—especially the removal of micro-fine inorganic ash from overflow concentrate. This work systematically evaluates the influences of ultrasonic parameters (power and treatment duration) and supergravity flow-field parameters (rotational speed and jet water pressure), and quantitatively compares macroscopic separation indices across different process stages. Microscopic morphological characterization via SEM further reveals particle morphological evolution and the underlying carbon–ash liberation mechanism triggered by ultrasonic pretreatment. This study provides fundamental experimental data and a feasible technical pathway for waste minimization and high-value resource utilization of coal gasification fine slag.

2. Materials and Methods

2.1. Materials

The coal gasification fine slag (CGFS) samples used in this study were obtained from a coal chemical enterprise in Yulin, Shaanxi Province, China. The received samples were subjected to proximate analysis, and the results are shown in Table 1. It can be observed that the fixed carbon content of the sample is 25.60%, indicating its recovery potential. Subsequently, X-ray fluorescence (XRF) tests were performed to analyze the chemical composition of the ashed 0.125–0.5 mm CGFS, and the results are presented in Table 2. It is found that its primary chemical constituents are SiO_2, Al_2O_3, Fe_2O_3 and CaO, with corresponding contents of 46.81%, 17.57%, 14.50% and 10.50%, respectively.

Table 1. Proximate analysis of received samples (wt%).

Component	Moisture	Ash	Volatiles	Fixed Carbon
Weight	1.03	68.31	5.06	25.60

Table 2. Main chemical composition of the ashed 0.125–0.5 mm CGFS (wt%).

Component	SiO_2	Al_2O_3	Fe_2O_3	CaO	Other
Weight	46.81	17.57	14.50	10.50	10.62

To clarify the particle size distribution of the samples used in the experiments, the particle size distribution of the CGFS was analyzed using a laser particle size analyzer, as presented in Figure 1. The CGFS exhibited a broad and continuous particle size distribution. The characteristic particle sizes (D10, D50, and D90) of the raw slag were 15.05 μm, 195.0 μm, and 494.7 μm, respectively, indicating a high proportion of fine and micro-fine particles. This broad particle size distribution highlights the inherent limitations of conventional physical separation methods. Consequently, the high proportion of these fine particles makes the effective liberation and recovery of residual combustible matter challenging, thereby indicating the need for an intensified combustible matter-ash separation process.

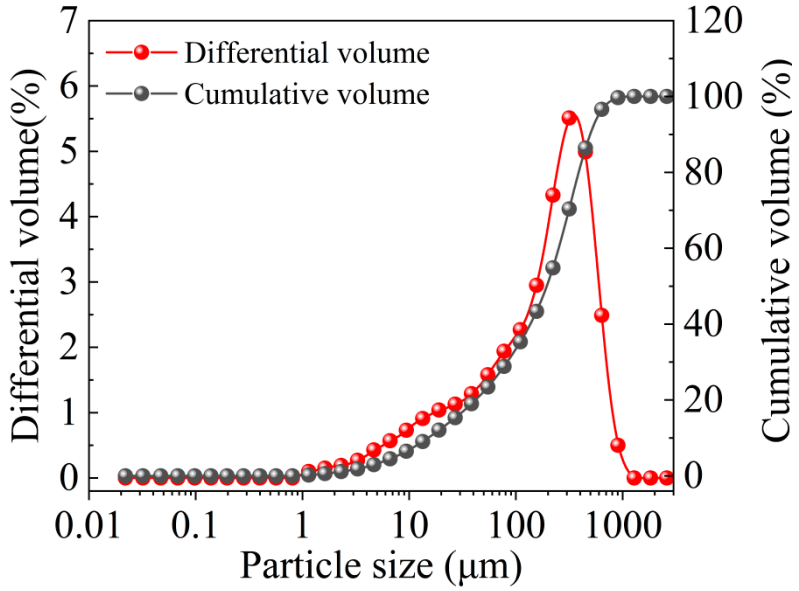


Figure 1. Particle size distribution of the raw CGFS sample.

2.2. Characterization Techniques

To compare the surface micro-morphology of the fine slag before and after separation, a Hitachi SU8600 scanning electron microscope (SEM) (Hitachi High-Tech Corporation, Tokyo, Japan) equipped with an Ultimax 40 energy-dispersive X-ray spectrometer (EDS) (Oxford Instruments plc, Abingdon, UK) was employed for morphological and compositional analyses.

2.3. Ultrasonic Pretreatment

The ultrasonic pretreatment experiments were conducted using a probe-type ultrasonic processor (Dawei Ultrasonic Equipment Co., Ltd., Xuzhou, China; operating frequency: 20 kHz). For each test, 50 g of the 0.125–0.5 mm CGFS sample was dispersed in water to prepare a suspension with a solids concentration of 100 g/L; the resulting suspension was then subjected to ultrasonic treatment. To investigate the effects of ultrasonic parameters, the ultrasonic power (20, 40, 60, 80, and 100 W) and processing time (30, 60, 90, 120, and 150 s) were varied while maintaining constant supergravity separation conditions (rotational speed of 472 r/min, jet water pressure of 0.03 MPa). The pretreated slurry was directly fed into the supergravity concentrator.

2.4. Supergravity Separation

A supergravity concentrator was employed for the separation of the 0.125–0.5 mm CGFS, and a schematic diagram of the equipment is shown in Figure 2. This apparatus primarily comprises a hollow rotating main shaft and an inverted porous drum. The backwash jet (a high-pressure water stream directed counter to the centrifugal force) is introduced into the water chamber via the hollow shaft, creating a pressure differential between the interior and exterior of the drum. This pressure differential forces the backwash jet to pass through the micro-holes on the drum wall into the separation chamber, establishing a stable, radially inward backwash flow field. The separation of fine slag particles within the device predominantly relies on the coupling effect of the supergravity field and the backwash jet: driven by settling differences in the intensified force field, high-density ash particles overcome the hydrodynamic resistance and settle outward to the underflow, while low-density carbon-rich particles migrate inward with the water flow into the overflow. The core operational parameters for the separation tests were jet water pressure and rotational speed, with specific settings detailed in Table 3. Upon completion of each separation trial,

the overflow (light product) and underflow (heavy product) were collected separately, dried, and subsequently used for weighing and loss on ignition (LOI) analysis.

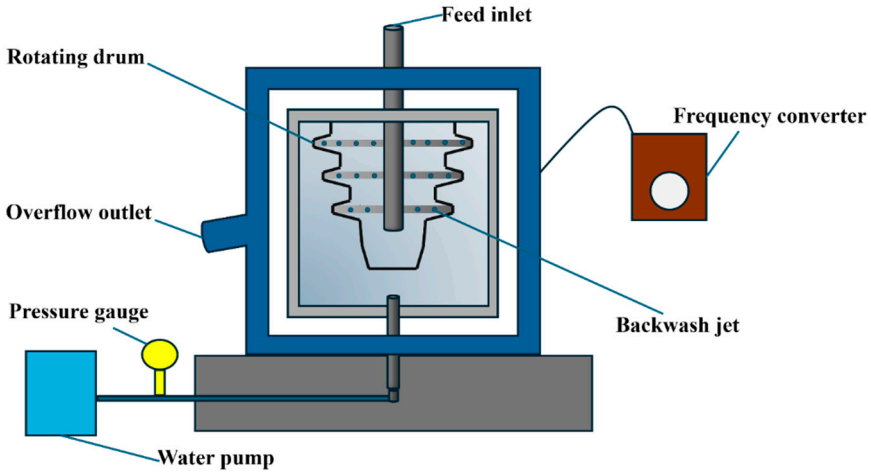


Figure 2. Schematic diagram of the supergravity separation system.

Table 3. Operating parameters for supergravity separation.

Parameters	Value
Feeding concentration (g/L)	100
Rotational speed (r/min)	236, 472, 708, 944, 1180
Jet water pressure (MPa)	0.01, 0.02, 0.03, 0.04, 0.05

2.5. Evaluation of Separation Effect

To objectively evaluate the separation performance under various conditions, the collected overflow products were dried and weighed. The ash contents of the feed and separation products were determined using a muffle furnace operated under a programmed slow-ashing procedure. The samples were subjected to a 150 min ashing cycle, followed by check ashing to verify the completeness of combustion. After cooling, the residual mass was measured to calculate the ash content. The concentrate yield $\boldsymbol{Y_c}$ and loss on ignition (LOI) were calculated based on Equations (1) and (2). Furthermore, Equation (3) was applied to evaluate the combustible recovery $\boldsymbol{R_c}$ of the concentrate. LOI was calculated as 100% minus the dry-basis ash content. Combustible recovery was calculated as the concentrate yield multiplied by the ratio of concentrate LOI to feed LOI.

$$\boldsymbol{Y_{c(\%)} = \frac{M_c}{M_f} \times 100\%} \quad (1)$$

$$\boldsymbol{LOI(\%) = 100\% - A} \quad (2)$$

$$\boldsymbol{R_{c(\%)} = \frac{M_c \times (100\% - A_c)}{M_f \times (100\% - A_f)} \times 100\%} \quad (3)$$

where $\boldsymbol{M_c}$ is the concentrate mass (g); $\boldsymbol{M_f}$ is the feed mass (g); $\boldsymbol{A_c}$ is the ash content of the concentrate (wt.%); $\boldsymbol{A_f}$ is the ash content of the feed (wt.%); and $\boldsymbol{A}$ represents the ash content in the corresponding separation product (wt.%).

3. Results and Discussion

3.1. Separation Results and Comparative Analysis

3.1.1. Optimization of Supergravity Separation Parameters

To ascertain the influence of supergravity flow field parameters on separation performance and establish baseline conditions for subsequent intensified processes, supergravity separation tests were initially conducted on raw slag without ultrasonic treatments. Figure 3 illustrates the contour distributions of the yield, loss on ignition (LOI), and combustible recovery of the overflow concentrate under various rotational speeds and jet water pressures.

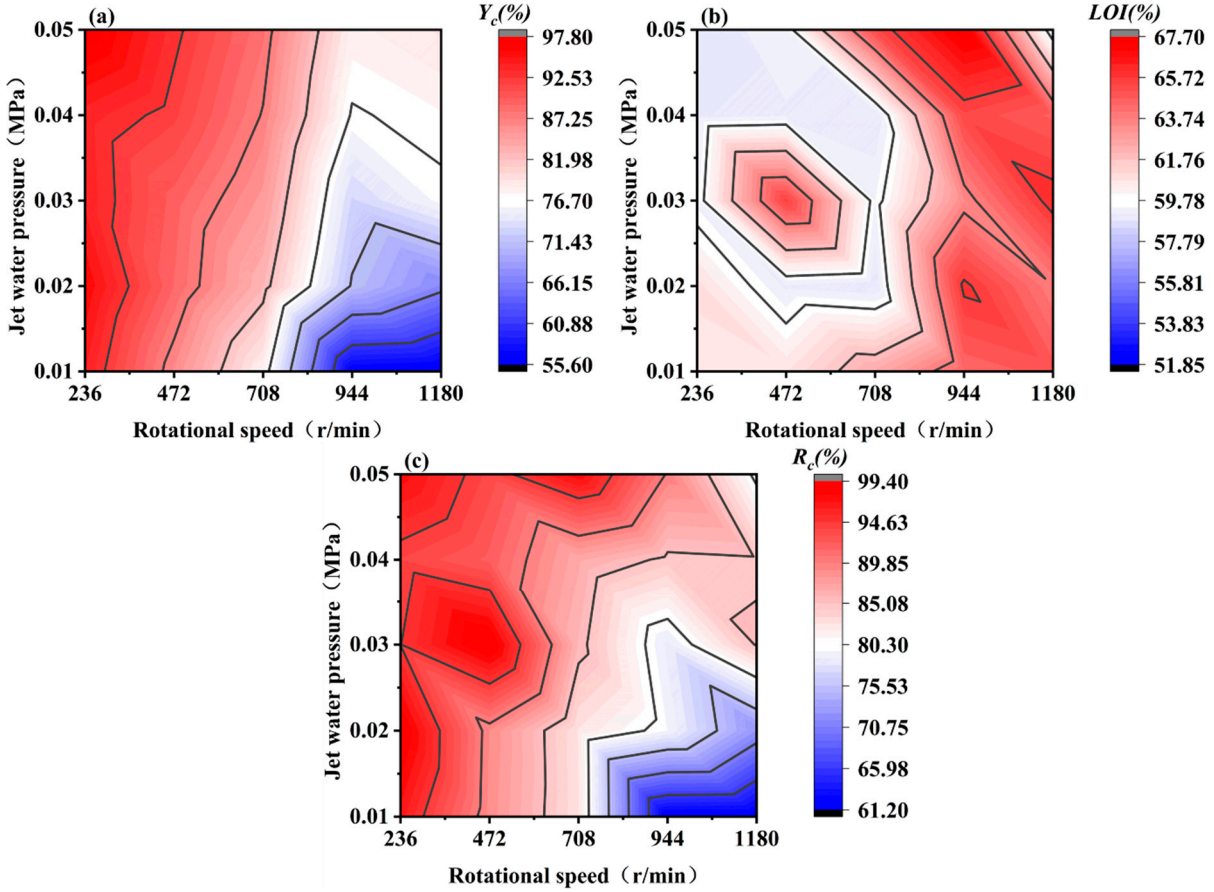


Figure 3. Effect of conventional supergravity separation parameters on the macroscopic separation indices of the concentrate ((**a**) yield; (**b**) loss on ignition; (**c**) combustible recovery).

As shown in Figure 3a, the concentrate yield fluctuated between 55.66% and 97.71%. The concentrate yield exhibited a gradual upward trend with the increase in jet water pressure, while it decreased with the increment of rotational speed. At low rotational speeds, the relatively high fluid resistance restricts the settling of high-density ash, leading to an elevated concentrate yield; conversely, high rotational speeds generate a stronger centrifugal force, promoting the settling of ash particles into the underflow and consequently reducing the yield. Meanwhile, an elevation in jet water pressure enhances the centripetal hydrodynamic traction, driving more particles into the overflow. Figure 3b indicates that the LOI of the conventionally separated concentrate was generally low (58.77–67.66%). This is attributed to the fact that a large amount of unliberated combustible matter-ash intergrowths in the fine slag may remain associated with combustible-rich particles and enter the overflow under the backwash effect [22,23]. Figure 3c demonstrates that the combustible recovery varied between 61.22% and 99.34%. At a rotational speed of 472 r/min and a jet water pressure of 0.03 MPa, the combustible recovery and LOI were 99.34% and

65.52%, respectively. Therefore, a rotational speed of 472 r/min and a jet water pressure of 0.03 MPa were established as the optimal baseline operating parameters for subsequent intensified separation experiments.

3.1.2. Determination of Ultrasonic Pretreatment Conditions

Under the optimal supergravity separation conditions, the effect of ultrasonic pretreatment conditions on the separation performance was further investigated. Figure 4 presents the effects of ultrasonic power and processing time on the loss on ignition (LOI) of the overflow concentrate.

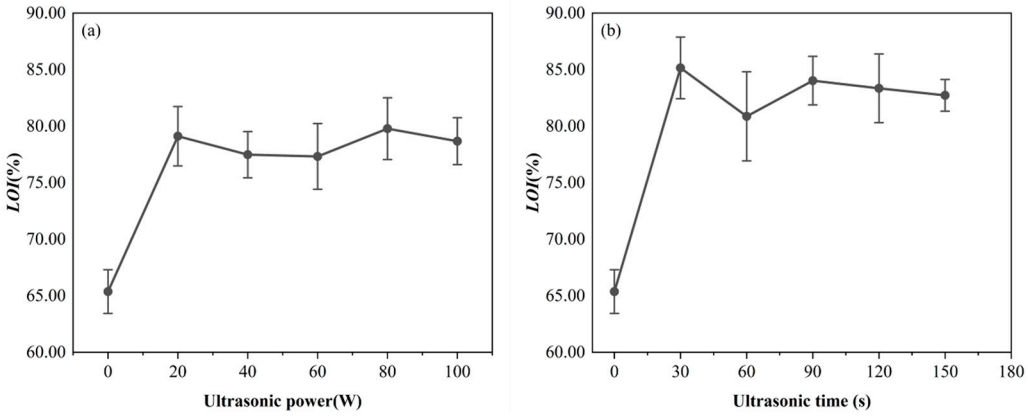


Figure 4. Effect of ultrasonic pretreatment parameters on the loss on ignition (LOI) of the overflow concentrate ((**a**) ultrasonic power, with treatment time fixed at 60 s; (**b**) ultrasonic time, with power fixed at 80 W). Common conditions: rotational speed, 472 r/min; jet water pressure, 0.03 MPa; CGFS particle size, 0.125–0.5 mm; feed solids concentration, 100 g/L.

As shown in Figure 4a, the influence of ultrasonic power on the separation efficiency was investigated. With the increase in ultrasonic power from 20 W to 100 W (at a fixed processing time of 60 s), the LOI of the overflow concentrate exhibited a trend of initially increasing and then decreasing, reaching its maximum value at 80 W. This suggests that a moderate ultrasonic energy input can promote cavitation-induced removal of the ash encapsulation layer from the particle surfaces; however, when the power exceeds 80 W within the tested range, the separation performance undergoes a notable deterioration instead. One possible explanation is that excessively high ultrasonic power may fragment the porous combustible skeleton, increasing fine-particle entrainment and reducing separation selectivity.

Figure 4b shows the effect of ultrasonic treatment time on concentrate quality. Under the condition of a fixed ultrasonic power of 80 W, as the ultrasonic processing time was extended from 30 s to 150 s, the concentrate LOI reached its highest level at 30 s and subsequently fluctuated below the 30 s peak. This time-dependent behavior suggests that an initial 30 s of sonication can promote removal of the ash layer. However, prolonged ultrasonic exposure may fragment the porous combustible matrix and alter the partitioning of fine particles during supergravity separation. Based on the peak LOI performance, 80 W and 30 s were ultimately selected as the optimal ultrasonic pretreatment conditions for the subsequent multi-process synergistic separation. Ren et al. reported ultrasonic fragmentation of carbon–ash composite particles before flotation [19], while Xue et al. associated ultrasound-assisted hydrophobic–hydrophilic separation with removal of ash from residual-carbon surfaces and pores [20]. These observations support a dispersion and cleaning role for pretreatment, although the optimum energy input and subsequent separation behavior depend on the feed and process.

3.1.3. Comparative Analysis of Multi-Process Synergistic Intensification Effects

To intuitively reveal the specific roles and synergistic intensification effects of ultrasonic pretreatment and sieving in the fine slag separation process, a comparative analysis of macroscopic separation indices was performed across four different operational scenarios under the previously determined optimal supergravity parameters (rotational speed of 472 r/min, jet water pressure of 0.03 MPa) and optimal ultrasonic conditions (power of 80 W, processing time of 30 s): scenario a (separation only), scenario b (ultrasound and separation), scenario c (separation and sieving), and scenario d (ultrasound, separation and sieving). The operating conditions are summarized in Table 4, and the corresponding results are illustrated in Figure 5.

Table 4. Operating conditions for the four processing scenarios.

Scenario	Ultrasonic Power (W)	Ultrasonic Time (s)	Rotational Speed (r/min)	Jet Water Pressure (MPa)	Wet Sieve Aperture (mm)
a	Not applied	Not applied	472	0.03	Not applied
b	80	30	472	0.03	Not applied
c	Not applied	Not applied	472	0.03	0.125
d	80	30	472	0.03	0.125

Note: "Not applied" indicates that the corresponding step was omitted.

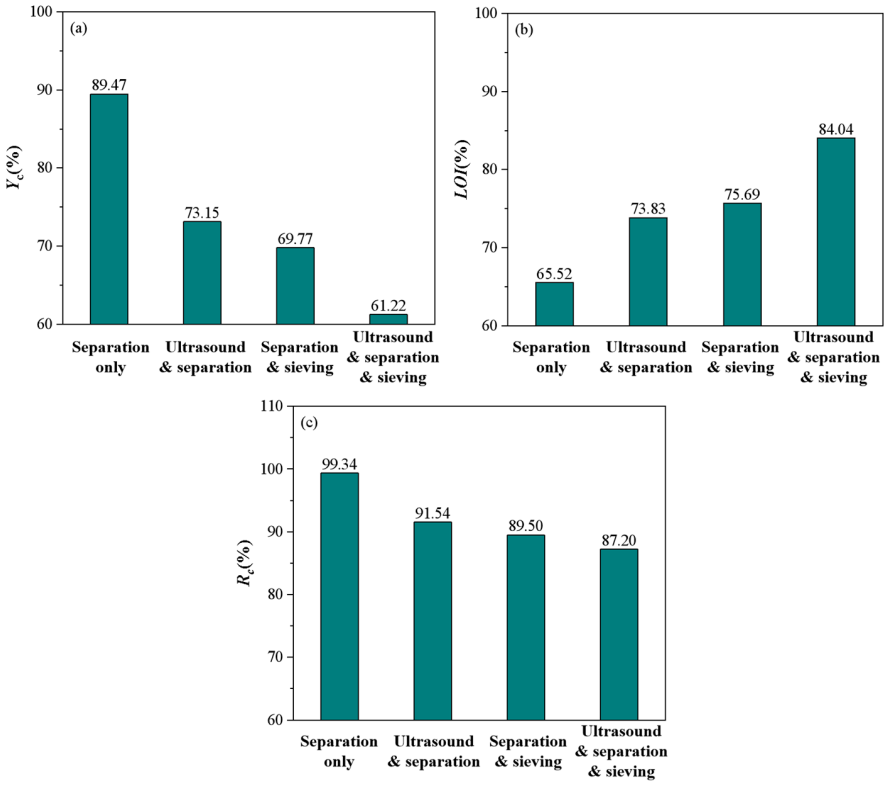


Figure 5. Effects of different operational scenarios on concentrate yield, loss on ignition (LOI), and combustible recovery ((**a**) yield; (**b**) loss on ignition; (**c**) combustible recovery).

Figure 5a depicts the variation characteristics of the overflow concentrate yield under different operational scenarios. It can be seen that with the progressive intensification of the separation process, the absolute concentrate yield exhibited a step-wise decreasing trend, sequentially declining from 89.47% in scenario a to 61.22% in scenario d. The high yield in scenario a may partly reflect the entrainment of ash-bearing particles and unliberated

combustible matter-ash aggregates. After introducing ultrasonic pretreatment (scenario b), cavitation-induced dispersion may dislodge the high-density glass microspheres deeply embedded within the porous skeleton of residual combustible matter. This may facilitate their partitioning into the underflow in the supergravity centrifugal field, resulting in a reduction in the overflow yield. The subsequent wet sieving operation (scenario d) can further remove this portion of free micro-fine ash. The sequential decrease in yield is consistent with the removal of ash-bearing material during the additional processing steps.

Figure 5b reveals the upgrading effect of step-wise process intensification on the concentrate loss on ignition (LOI). The results indicate that the concentrate LOI exhibited a significant increasing trend with the progressive intensification of processing conditions. When employing supergravity separation alone (scenario a), the concentrate LOI remained at a low level of 65.52%, indicating that physical upgrading encountered a severe precision bottleneck. Upon introducing ultrasonic pretreatment (scenario b) or single sieving (scenario c), the concentrate LOI was upgraded to 73.83% and 75.69%, respectively. Ultimately, when the combined ultrasound-supergravity-sieving process was adopted (scenario d), the concentrate LOI increased to a peak of 84.04%. A possible explanation for this increase in LOI is that ultrasonic cavitation promotes dispersion of combustible matter-ash aggregates and partial liberation of ash-bearing particles. This is subsequently coupled with the auxiliary washing effect of 0.125 mm wet sieving, which can reduce fine-slime entrainment into the concentrate. These complementary steps improve the final concentrate quality compared with supergravity separation alone.

Figure 5c illustrates the impact of different operational scenarios on the combustible recovery of the concentrate. As observed from Figure 5c, with the continuous intensification of the processing conditions, the combustible recovery exhibited a gradually decreasing trend. Under supergravity separation alone (scenario a), the combustible recovery reached its maximum value of 99.34%. With the incorporation of ultrasonic pretreatment and sieving stages, the recovery began to decline, reaching its minimum value of 87.20% under the combined ultrasound-supergravity-sieving process (scenario d). One possible explanation for this downward trend in recovery is that, on the one hand, while the mechanical vibrations generated by ultrasound break the encapsulation structure of heterogeneous agglomerates, they may also induce secondary sliming of the loosely structured residual combustible matter skeleton. These dislodged micro-fine combustible particles experience altered force balances within the supergravity field, potentially contributing to combustible matter loss in the underflow. On the other hand, this portion of liberated ultra-fine combustible particles may pass through the screen and be lost with the water flow during the subsequent 0.125 mm wet sieving stage. Correlating the concentrate LOI with the combustible recovery, a typical grade-recovery trade-off is observed. Although the combined steps of ultrasonic pre-dispersion and wet sieving inevitably result in a certain reduction in combustible recovery, they can alleviate the effects of fine ash entrainment. Consequently, this synergistic action effectively enhances the separation selectivity and the overall upgrading efficiency of the supergravity process. Li et al. showed that pre-sieving and flow-field regulation affected CGFS enrichment and entrainment in a dry centrifugal classifier [21]. In a wet system, Liu et al. found that sieving combined with water-flow classification improved carbon enrichment [24]. Collectively, these results demonstrate the influence of size-specific sieving on separation performance.

3.2. Separation Mechanism of the Ultrasonic Dispersion-Enhanced Supergravity-Sieving Process

To reveal the evolution of particle micro-morphology and the combustible matter-ash separation mechanism across different process stages of the ultrasonic dispersion-enhanced supergravity-sieving process, scanning electron microscopy (SEM) tests were conducted

on the raw fine slag, ultrasound-only sample, supergravity-only sample, and the final concentrate obtained from the combined process.

3.2.1. Evolution of Particle Micro-Morphology

The intensification mechanism of ultrasonic pretreatment primarily stems from the localized high-pressure shock waves and strong mechanical shear forces induced by the ultrasonic cavitation effect [25]. To intuitively reveal the influence of these effects on the micro-liberation characteristics of fine slag particles, Figure 6 compares the SEM surface morphologies of samples under different processing conditions (the left side shows the low-magnification panorama at 5000×, and the right side corresponds to the high-magnification localized view at 20,000× within the red dashed box). As shown in Figure 6a, in the untreated raw fine slag, irregular porous residual combustible matter is tightly adhered to a large amount of micro-fine ash, forming a robust heterogeneous agglomerate structure. High-magnification observation further shows that a large number of spherical glass microspheres are not only attached to the surface of combustible particles but are also deeply embedded and packed within the internal pores of the residual combustible matter. Such physical encapsulation may influence the settling behavior of composite particles and hinder separation based on the density differences between the individual components. Figure 6b presents the micro-morphology of the overflow product after supergravity separation alone. Although the loose attachments on the surface of large combustible particles decreased under fluid backwash erosion, a large number of aggregated glass microspheres are still embedded within their deep grooves and pores. These observations suggest that supergravity separation alone may be insufficient to remove ash associated with combustible-rich particles, which could contribute to the low concentrate LOI.

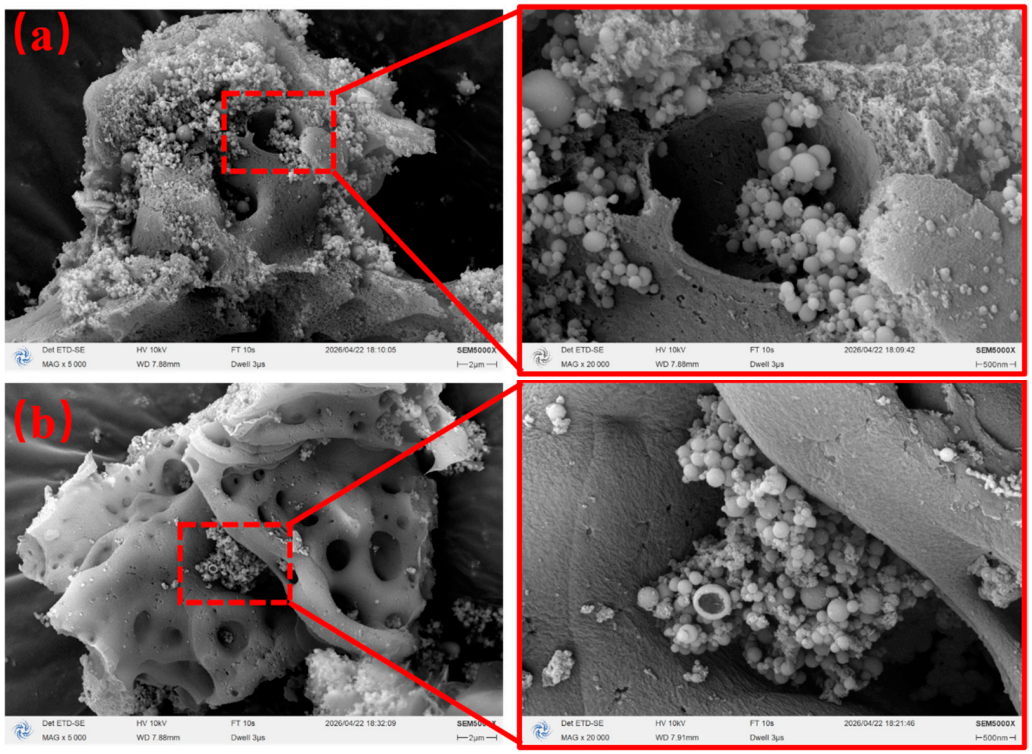


Figure 6. *Cont.*

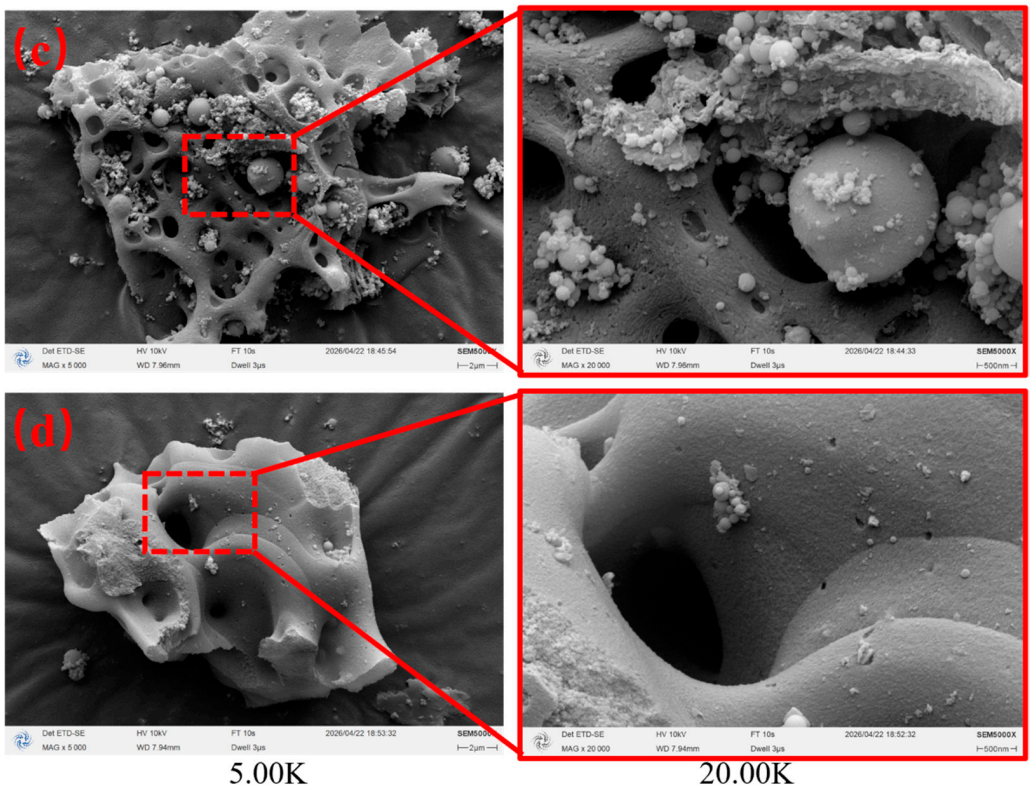


Figure 6. SEM micro-morphologies of fine slag particles under different processing conditions ((**a**) raw sample; (**b**) separation only; (**c**) ultrasound only; (**d**) ultrasound, separation and sieving).

After introducing ultrasonic pretreatment, the micro-dispersion state of the particles changed. As shown in the "ultrasound only" sample in Figure 6c, the ultrasonic cavitation effect significantly disrupted the heterogeneous agglomeration state, and the micro-fine ash contamination layer on the surface of combustible particles was stripped over a large area in the low-magnification view. The high-magnification morphology shows fewer embedded glass microspheres in the observed surface regions and more discrete particles, suggesting partial dispersion of the original aggregates. However, due to the lack of a subsequent separation flow field, the liberated ash remained mixed within the system. Previous CGFS flotation studies likewise show that particle conditioning influences separation performance [26], although their reagent and hydrodynamic conditions differ from those used here.

Figure 6d displays the morphology of the final overflow concentrate after the combined ultrasound-supergravity processing and sieving (+0.125 mm). At this stage, the surface of the residual combustible matter is cleaner, with its well-developed porous skeleton structure more clearly exposed, and free glass microspheres are rarely detected inside the pores. This morphological evolution suggests that the combined process clears the contamination layer on the combustible-particle surface and weakens the agglomeration effect through physical liberation, which may facilitate subsequent particle separation. Liberated high-density glass microspheres and fine ash particles may partition into the underflow under the centrifugal force field, reducing the entrainment of non-carbonaceous components in the overflow. This microscopic evidence is consistent with the measured decrease in concentrate yield and increase in LOI under the combined process.

3.2.2. Element Distribution and Content Analysis on Particle Surfaces

To further reveal the liberation mechanism and intensification effect of ultrasonic pretreatment on the combustible matter-ash heterogeneous agglomerates, EDS elemental

mapping and point spectrum analysis were employed to investigate the spatial distribution and weight percentage (wt%) evolution of elements on the surfaces of fine slag particles at different processing stages. Figure 7 presents the corresponding qualitative and quantitative analysis results.

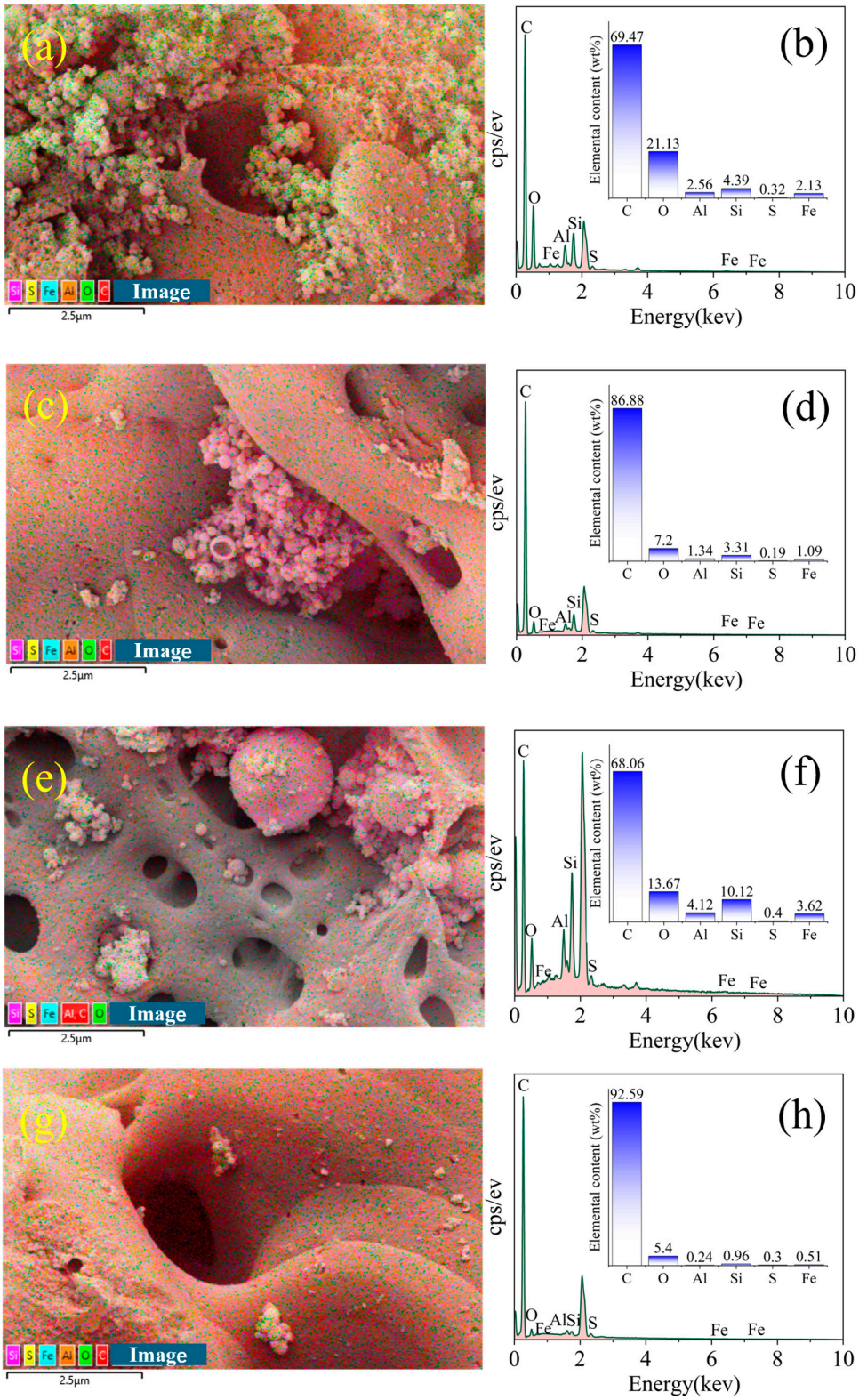


Figure 7. Comparison of SEM morphologies and EDS spectra of fine slag particles under different processing conditions: (**a**,**b**) raw sample; (**c**,**d**) separation only; (**e**,**f**) ultrasound only; (**g**,**h**) ultrasound, separation and sieving.

As shown in Figure 7a,b, the surface of the untreated raw fine slag is densely covered by a large amount of inorganic ash elements, where the C element signal heavily overlaps with inorganic ash signals such as Si and Al in space. Combined with the quantitative EDS analysis, the carbon content in the surface micro-region is 69.47 wt%, while the Si content is 4.39 wt%. This suggests that the residual combustible matter matrix of the gasification fine slag is heavily encapsulated by the inorganic mineral layer.

Figure 7c,d depict the element distribution characteristics of the overflow concentrate after supergravity separation alone. The results indicate that the carbon content in the surface micro-region increased to 86.88 wt%, and some surface impurities were effectively washed away. However, combined with the macroscopic separation data in Section 3.1 (where the overall LOI of the concentrate remained relatively low without pretreatment), a significant discrepancy between local elemental carbon measurements and bulk combustible content was observed in this sample. One possible explanation is that EDS characterizes a localized interaction volume, whereas bulk LOI represents the overall product; the two measurements are therefore not directly equivalent. These observations suggest that single hydrodynamic backwash erosion may be insufficient to completely separate deep-seated, high-density inorganic impurities, thereby limiting the improvement of separation precision.

After the introduction of ultrasonic pretreatment, the micro-region element distribution exhibited a crucial evolutionary pattern. As shown in the "ultrasound only" sample in Figure 7e,f, the changes in elemental distribution may be associated with ultrasonic dispersion of ash-bearing aggregates. In the absence of a subsequent supergravity separation step, the analyzed surface micro-region showed a higher Si content (10.12 wt%) than the raw sample (4.39 wt%). This local elemental enrichment is consistent with changes in the distribution of ash-associated material, although EDS alone cannot establish a specific ash-migration pathway.

Figure 7g,h present the chemical composition characteristics of the final overflow concentrate following ultrasound-enhanced supergravity separation and sieving (+0.125 mm). Ultrasonic dispersion followed by centrifugal settling, backwash flow and wet sieving may promote removal of ash-bearing particles. At this stage, the elemental map is dominated by a highly continuous and dense C element distribution, with almost no interference from inorganic elements; the quantitative data show that the measured C content in the analyzed surface micro-region reached 92.59 wt%, consistent with a carbon-rich surface, while the residual amounts of inorganic ash elements such as Si (0.96 wt%) and Al (0.24 wt%) are extremely low. These EDS observations, together with the bulk LOI results, support enrichment of residual combustible matter by the combined process.

4. Conclusions

(1) SEM micro-characterization suggested that ultrasonic pretreatment promoted dispersion of the heterogeneous agglomerates in CGFS. This process reduced the micro-fine ash contamination layer on the combustible-particle surface, consistent with partial liberation of combustible matter-ash aggregates.

(2) The optimal ultrasonic pretreatment operating window was established at a power of 80 W and a processing time of 30 s. Under these conditions, the combined ultrasound-supergravity-sieving process improved concentrate quality. Compared with direct separation without pretreatment, the loss on ignition (LOI) of the final concentrate increased substantially from 65.52% to 84.04%.

(3) To address the issue of fine ash entrainment, coupling a 0.125 mm wet sieving stage proved essential for final product purification. Through this multi-stage physical intensification process, a high-grade concentrate was ultimately obtained with a yield of

61.22% and a combustible recovery of 87.20%, confirming the deep intensification potential of the ultrasonic dispersion-enhanced supergravity-sieving strategy for upgrading residual combustible matter quality.

Author Contributions: J.H.: Methodology, Funding acquisition, Supervision, Writing—review & editing. L.Y.: Validation, Investigation, Writing—original draft. Y.Z.: Methodology, Formal analysis, Supervision. L.Z.: Funding acquisition, Writing—review & editing. Y.L.: Methodology, Visualization. All authors have read and agreed to the published version of the manuscript.

Funding: This work was supported by the National Natural Science Foundation of China (No. 52274280), the Open Foundation of State Key Laboratory of Mineral Processing (No. BGRIMM-KJSKL-2025-13), the China Postdoctoral Science Foundation (No. 2025M781750), the Postdoctoral Fellowship Program of China Postdoctoral Science Foundation (CPSF) under Grant GZC20261042.

Data Availability Statement: The original contributions presented in this study are included in the article. Further inquiries can be directed to the corresponding author.

Conflicts of Interest: The authors declare no conflicts of interest.

Abbreviations

The following abbreviations are used in this manuscript:

CGFS	Coal gasification fine slag
LOI	Loss on ignition
SEM	Scanning electron microscope
EDS	Energy Dispersive Spectrometer

References

1. Guo, F.; Guo, Y.; Chen, L.; Jia, W.; Zhu, Y.; Li, Y.; Wang, H.; Yao, X.; Zhang, Y.; Wu, J. Multitudinous components recovery, heavy metals evolution and environmental impact of coal gasification slag: A review. *Chemosphere* **2023**, *338*, 139473. [CrossRef] [PubMed]
2. Zhao, X.; Yang, K.; Yuan, L.; He, X.; Chi, X. Widespread quantitative assessment for potential environmental risk of heavy metals in coal gasification slag from China. *Ecotoxicol. Environ. Saf.* **2025**, *297*, 118235. [CrossRef] [PubMed]
3. Zhao, X.; Zeng, C.; Mao, Y.; Li, W.; Peng, Y.; Wang, T.; Eiteneer, B.; Zamansky, V.; Fletcher, T. The Surface Characteristics and Reactivity of Residual Carbon in Coal Gasification Slag. *Energy Fuels* **2010**, *24*, 91–94. [CrossRef]
4. Wu, Y.; Liu, C.; Ma, Y.; Sun, Y.; Ji, W.; Zhu, L.; Bai, H. One step reconstruction of carbon/P zeolite from coal gasification slag and its adsorption mechanism for crystal violet. *J. China Coal Soc.* **2025**, *50*, 2658–2670. [CrossRef]
5. Liu, X.; Jin, Z.; Jing, Y.; Fan, P.; Qi, Z.; Bao, W.; Wang, J.; Yan, X.; Lv, P.; Dong, L. Review of the characteristics and graded utilisation of coal gasification slag. *Chin. J. Chem. Eng.* **2021**, *35*, 92–106. [CrossRef]
6. Ren, L.; Ding, L.; Guo, Q.; Gong, Y.; Yu, G.; Wang, F. Characterization, carbon-ash separation and resource utilization of coal gasification fine slag: A comprehensive review. *J. Clean. Prod.* **2023**, *398*, 136554. [CrossRef]
7. Yu, W.; Zhang, H.; Wang, X.; Rahman, Z.U.; Shi, Z.; Bai, Y.; Wang, G.; Chen, Y.; Wang, J.; Liu, L. Enrichment of residual carbon from coal gasification fine slag by spiral separator. *J. Environ. Manag.* **2022**, *315*, 115149. [CrossRef] [PubMed]
8. Liu, B.; Lv, P.; Mai, D.; Bai, Y.; Wang, J.; Su, W.; Song, X.; Yu, G. Investigation of particle size effects and interfacial interaction mechanisms during froth flotation of coal gasification fine slag. *Fuel* **2026**, *420*, 139007. [CrossRef]
9. Chen, R.; Wang, H.; Yang, M.; Yan, X.; Ran, J.; Zhang, H. Pilot-scale experiment and numerical simulation of deep flotation of coal gasification fine slag. *Process Saf. Environ. Prot.* **2026**, *213*, 109009. [CrossRef]
10. Wang, S.; Kadagala, M.R.; Vinnett, L.; Sharma, N.K.; Wei, G. Investigation on a novel mixed collector for carbon recovery from coal gasification fine slag: Experimental insight and macro molecular simulations. *Powder Technol.* **2025**, *451*, 120473. [CrossRef]
11. Han, R.; Zhou, A.; Zhang, N.; Li, Z.; Cheng, M.; Chen, X.; Nan, T. Effective separation of coal gasification fine slag: Role of classification and ultrasonication in enhancing flotation. *Int. J. Min. Sci. Technol.* **2024**, *34*, 867–880. [CrossRef]
12. Fan, X.; Fan, P.; Ren, Z.; Liu, X.; Bao, W.; Wang, J.; Dong, L.; Fan, M. Separation and physicochemical properties of residual carbon in gasification slag. *Physicochem. Probl. Miner. Process.* **2022**, *58*, 154928. [CrossRef]
13. Lv, B.; Chai, X.; Deng, X.; Jiao, F.; Fang, C.; Xing, B. Recovery of residual carbon from coal gasification fine slag by a combined gravity separation-flotation process. *J. Environ. Manag.* **2023**, *348*, 119351. [CrossRef] [PubMed]

14. Jiao, Y.; Yang, Z.; Han, X.; Wang, K.; Fang, C.; Zhao, Z.; Tang, W. Ultrasonication Improves the Flotation of Coal Gasification Fine Slag Residue. *Minerals* **2024**, *14*, 363. [CrossRef]
15. Sun, M.; Gu, S.; Liu, D.; Xu, Z.; Wang, W.; Tu, Y.; Wang, L.; Liu, H.; Lu, S. Enrichment of Residual Carbon in Coal Gasification Fine Slag via Wet Sieving Separation with Ultrasonic Pretreatment. *ACS Omega* **2022**, *7*, 40306–40315. [CrossRef] [PubMed]
16. Mao, Y.; Chen, Y.; Bu, X.; Xie, G. Effects of 20 kHz ultrasound on coal flotation: The roles of cavitation and acoustic radiation force. *Fuel* **2019**, *256*, 115938. [CrossRef]
17. Kundu, T.; Dash, N.; Angadi, S.I. Separation behavior of Falcon concentrator for the recovery of ultrafine scheelite particles from the gold mine tailings. *Sep. Purif. Technol.* **2023**, *309*, 123065. [CrossRef]
18. Silva, G.V.; Oliveira, G.J.R.; Horta, D.G. Effect of ultrasonic pre-treatment on the reverse flotation of kaolinite from bauxite. *Miner. Process. Extr. Metall. Rev.* **2024**, *45*, 982–990. [CrossRef]
19. Ren, L.; Gong, Y.; Guo, Q.; Yu, G. Enhanced flotation of coal gasification fine slag based on ultrasonic pretreatment pulp and composite collector. *Powder Technol.* **2023**, *424*, 118530. [CrossRef]
20. Xue, Z.; Gao, F.; Dong, L.; Bao, W.; Wang, J.; Fan, P. Promotion of hydrophobic-hydrophilic separation of coal gasification fine slag through ultrasonic pre-treatment. *J. Environ. Chem. Eng.* **2023**, *11*, 110653. [CrossRef]
21. Li, L.; Li, X.; Zhang, Q.; Ma, S.; Peng, Z.; Han, C.; Lian, W.; Gao, C.; Li, P.; Huang, W. Innovative centrifugal airflow upgrading for coal gasification fine slag based on experiment and CFD-DEM approach. *Powder Technol.* **2024**, *447*, 120197. [CrossRef]
22. Tang, H.; He, J.; Fu, L.; Zhang, J.; Yao, L.; Yang, B.; Zhu, L.; Guo, S. Supergravity separation: An innovative strategy for efficient cleaning and upgrading of coal gasification slag waste. *Waste Manag.* **2025**, *205*, 114973. [CrossRef] [PubMed]
23. Fan, P.; Ge, Z.; Ren, Z.; Bao, W.; Wang, J.; Dong, L.; Fan, M. Experimental research and mechanism analysis of combined gravity-magnetic separation on coal gasification fine slag. *Int. J. Coal Sci. Technol.* **2025**, *12*, 81. [CrossRef]
24. Liu, Y.; Zhang, Q.; Li, L.; Wang, H.; Zhi, P.; Zhang, B.; Yang, M.; Shi, P.; Huang, W. Washability evaluation of coal gasification slag via an integrated sieving-water flow classification. *Waste Manag.* **2026**, *219*, 115551. [CrossRef] [PubMed]
25. Zhang, H.; Du, M.; Hu, H.; Zhang, H.; Song, N. A Review of Ultrasonic Treatment in Mineral Flotation: Mechanism and Recent Development. *Molecules* **2024**, *29*, 1984. [CrossRef] [PubMed]
26. Liang, Y.; Wang, H.; Chen, R.; Li, D.; Tian, Q.; Li, L.; Zhang, H. Intensification of flotation separation process of residual carbon from coal gasification fine slag using ultrafine carbon particles conditioning. *Int. J. Coal Prep. Util.* **2024**, *44*, 2044–2059. [CrossRef]

Disclaimer/Publisher's Note: The statements, opinions and data contained in all publications are solely those of the individual author(s) and contributor(s) and not of MDPI and/or the editor(s). MDPI and/or the editor(s) disclaim responsibility for any injury to people or property resulting from any ideas, methods, instructions or products referred to in the content.